Behavior of an Organic Solvent Drop During the Supercritical Extraction of Emulsions

Facundo Mattea
High Pressure Processes Group, Dept. of Chemical Engineering and Environmental Technology, University of Valladolid, Valladolid 47011, Spain

Universidad de Valladolid, Facultad de Ciencias, Prado de la Magdalena s/n, Valladolid 47011, Spain

Ángel Martín
High Pressure Processes Group, Dept. of Chemical Engineering and Environmental Technology, University of Valladolid, Valladolid 47011, Spain

Universidad de Valladolid, Facultad de Ciencias, Prado de la Magdalena s/n, Valladolid 47011, Spain

Lehrstuhl für Verfahrenstechnische Transportprozesse, Ruhr Universität Bochum, Universitätsstraße 150, 44801 Bochum, Germany

Constantin Schulz, Philip Jaeger, and Rudolf Eggers
Technical University Hamburg-Harburg, Process Engineering II, Heat and Mass Transfer, Ei*ß*endorfer Str. 38, 21073, Hamburg, Germany

María José Cocero
High Pressure Processes Group, Dept. of Chemical Engineering and Environmental Technology, University of Valladolid, Valladolid 47011, Spain

Universidad de Valladolid, Facultad de Ciencias, Prado de la Magdalena s/n, Valladolid 47011, Spain

DOI 10.1002/aic.12061
Published online October 23, 2009 in Wiley InterScience (www.interscience.wiley.com).

*The behavior of a drop of dichloromethane in water in contact with CO_2 at high pressure has been investigated with the purpose of analyzing the phenomena that takes place during the supercritical fluid extraction of emulsions process. Experiments have been performed with and without a solute (β-carotene) and a surfactant (*n*-octenylsuccinic anhydride-modified starch) dissolved in the drop, and the evolution of the drop volume as well as of the interfacial tension between the drop and the aqueous phase has been measured. Additionally, a mathematical model has been developed that allows describing the mass transfer. Results show that the drop undergoes swelling and shrinking processes due to diffusion of CO_2 into the drop and dichloromethane out of the drop. CO_2 concentration in the drop can be as high as 0.9 (molar fraction). Emulsion drops behave as miniature gas antisolvent precipitators and many particles are formed inside the drop. The interfacial tension between the drop and the aqueous*

Additional Supporting Information may be found in the online version of this article.

Correspondence concerning this article should be addressed to Á. Martín at mamaan@iq.uva.es

© 2009 American Institute of Chemical Engineers

phase increases during the process, therefore destabilizing the emulsion. © 2009 American Institute of Chemical Engineers *AIChE J,* 56: 1184–1195, 2010
Keywords: interfacial tension, supercritical carbon dioxide, β-carotene, n-*octenyl succinic anhydride (OSA)-modified starch, image analysis*

Introduction

The production of pharmaceutical and food particles in the nanometer size has been studied in the past years.[1] Particles in the nanometer scale present several advantages over the micrometer scale analogues: dissolution rates are enhanced due to the huge increase in superficial area,[2,3] suspensions stability is also higher and even the solubility of some compounds can be enhanced when particle size is in the nanometer scale.[4]

Natural substances with health benefits are of great interest for the nutraceutical and food industries. Carotenes have antioxidant effects, colorant properties, and β-carotene and other carotenes are vitamin A precursors in the human organism.[4] Despite all these benefits, carotenoids have a very low solubility in water and for their industrial application as colorants in aqueous media it is necessary to formulate them as a suspension with a small enough particle size.[5] The production of particulate systems of carotenoids to overcome these difficulties has been recently reviewed.[6] In particular, it has been shown that when supercritical antisolvent coprecipitation techniques are applied to the formulation of carotenoids, it is difficult to reduce particle size below the micrometer range.[7,8] A new promising technology to produce nanometer particles of natural substances is the use of supercritical fluids in combination with nanoemulsions, which presents advantages over these two separated technologies. This process, denominated supercritical fluid extraction of emulsions (SFEE),[9] consists in extracting the organic solvent from the droplets of an oil-in-water emulsion by using supercritical carbon dioxide. If a solute is dissolved in the organic solvent, the extraction causes the precipitation of the solute. Several authors have already applied this process[9–11] obtaining a relationship between the original drop size distribution present in the emulsion and the final particle sizes obtained in the precipitation process. Thus, a major advantage of the SFEE process over other supercritical precipitation techniques is the possibility of modifying the final particle size by changing the droplet size of the emulsion.

To obtain a better comprehension of the phenomena occurring during the precipitation process, the present research work intends to elucidate what happens within a drop of dispersed phase while the precipitation process is being carried out. For that purpose, a single drop of organic solvent was immersed in an aqueous medium inside a high-pressure visual cell and carbon dioxide was introduced at a desired pressure. The evolution of the drop was followed with the aid of a CCD-camera. The system dichloromethane-water-carbon dioxide has been studied to obtain a better comprehension of the precipitation process of β-carotene of a DCM-H_2O emulsion in the SFEE process. The evolution of a drop containing β-carotene and a drop of DCM in a surfactant solution under CO_2 pressure has also been studied. The variation in the interfacial tension between the continuous aqueous phase and the organic phase drops during CO_2 transfer has also been measured with the pendant drop method. Additionally, a mathematical model of the diffusion and phase equilibrium in this system has been elaborated to complement experimental results.

Materials and Methods

Materials

The liquids used in this work to prepare the emulsions are deionized water and dichloromethane (>99.9%) provided by Merck, Germany. An *n*-octenylsuccinic anhydride (OSA)-modified starch was used as emulsifier agent. This OSA-starch was obtained free of charge from National Starch Food Innovation (Hamburg, Germany). Crystalline β-carotene with a minimum purity of 99% was kindly provided by Vitatene SA (León, Spain). Carbon dioxide (99.5%) was purchased from Westfalen Gas, Germany.

Methods

Experimental setup. The experimental setup for the sessile drop and the pendant drop method can be seen in Figure 1.

It consists of a high pressure view-cell with two opposing windows. The view-cell has a volume of 300 mL and is designed for a maximum pressure of 30 MPa and a maximum temperature of 353 K. Inside the view-cell, a glass

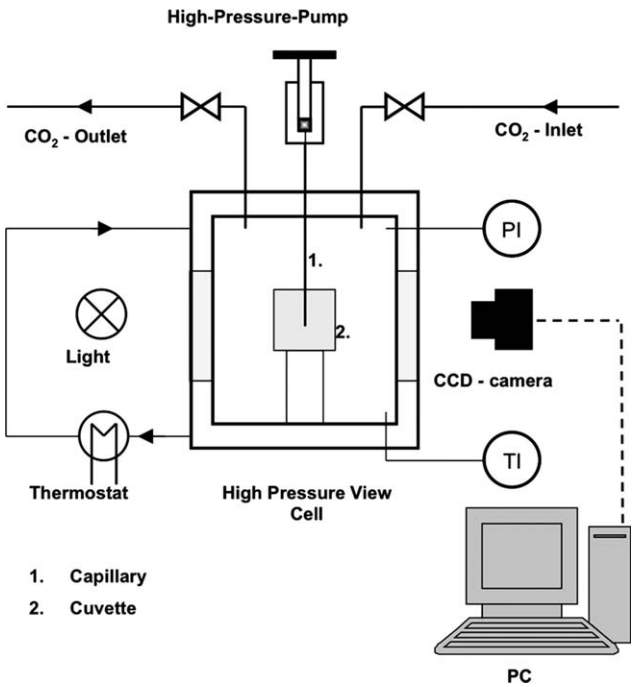

Figure 1. Experimental setup for the sessile and pendant drop methods.

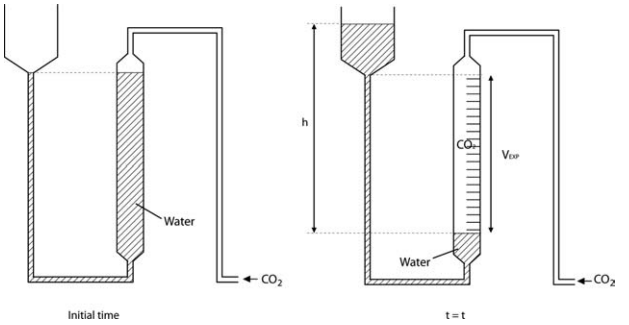

Figure 2. Experimental setup for the measurement of the amount of CO_2 dissolved in the droplet by volume displacement.

cuvette, purchased from Hellma Germany, with an inner volume of 6 mL is placed, which contains the aqueous phase. The interfacial area between the aqueous phase and the CO_2 phase is 400 mm^2. To introduce the dichloromethane, a capillary with an outer diameter of 0.5 mm is installed from the top of the cell. Pendant drops of dichloromethane can be formed by using a high-pressure pump at the upper part of the capillary. Sessile drops are formed outside the cell at the bottom of the cuvette. Cell temperature is kept constant by an external thermostat and is measured by a thermocouple with an accuracy of ± 0.1°C. Pressure was measured with pressure gauges with an accuracy of 0.4 MPa. For the optical evaluation of the drop, a CCD-camera was installed at one window of the cell. The images of the camera were recorded by a computer and later evaluated with an image processing software called "drop shape analysis" (DSA) provided by Krüss GmbH, Germany.

For determining the composition of the dichloromethane rich phase during the experiment, the high-pressure pump is exchanged to a gas sampling pipe at the upper part of the capillary before pressurization. The sample mass is then determined by weighing the gas sampling pipe. To measure the CO_2 content in the sample, the gas sampling pipe is connected to a system of communicating pipes (see Figure 2). The amount of CO_2 can be calculated by measuring the displacement of water in the first pipe. A cool trap is used to ensure the condensation of dissolved dichloromethane in the evaporated CO_2.

Experimental procedures

Before beginning an experiment, water and dichloromethane were mixed and thermostated at the same temperature of the experiment to obtain saturated aqueous and organic phases. This was done to avoid mass transfer of dichloromethane and water between the droplet and the continuous aqueous phase before the pressurization with carbon dioxide.

Two types of experiments were performed: the study of the evolution of drop volume after pressurization with CO_2, which was done with the objective of characterizing mass transfer in this system; and the study of the variation of the interfacial tension between the organic and aqueous phase in contact with CO_2 at high pressure. Preliminary tests performed using the pendant droplet method (suspending an organic phase droplet from a capillary inside the continuous aqueous phase) demonstrated that experiments were perturbed by random spills of fresh dichloromethane from the capillary inside the pendant droplet, probably caused by the decrease of the density of the droplet due to the dissolution of CO_2. Therefore, the sessile drop method (placing the organic phase drop on the bottom of the cell) was preferred for the experiments performed for determining the drop volume variation. This type of experiments is possible in this case because the density of dichloromethane (1.33 g/mL) is higher than that of water. The pendant drop method had to be used for interfacial tension determinations as required by the measurement method, which consists of calculating the interfacial tension from the shape of the pendant drop as described later.

With the sessile drop method, the drop was previously formed inside the aqueous medium and placed at the bottom of the cell. Initial size of the drops was varied between 5 and 20 μL. Once that the temperature of the sample was stabilized at the desired value CO_2 was injected into the cell. Pressure was slowly increased over a period of several minutes to avoid excessive stirring of the aqueous phase by the gas, which would cause a nonreproducible convective mass transfer of CO_2 into the fluid. After reaching the desired pressure, the evolution of the drop was recorded by means of a CCD-camera and the obtained images were analyzed with the aid of an image processing software called DSA provided by Krüss GmbH. The drop shape and volume was calculated with the image analysis software taking as a reference for size determinations the known diameter of the capillary used to introduce the drop into the cell, as it is shown in Figure 2.

For the determination of interfacial tension with the pendant drop method, the aqueous medium was first pressurized with CO_2 and once the desired operative conditions were met, a drop of the dichloromethane rich phase was formed at the tip of the capillary placed inside the cell. The evolution of the experiment was recorded and with the aid of the DSA software, the shape of the drop was related to the interfacial tension between both phases, using the pendant drop fundamental equation according to Bashforth and Adams (Eq. 1).[12] This equation can be used to relate the interfacial tension and densities of the coexisting phases with pure geometrical parameters of the surface determined by the image analysis software. Figure 3 shows an example of the correlation of drop shape performed by the image analysis software.

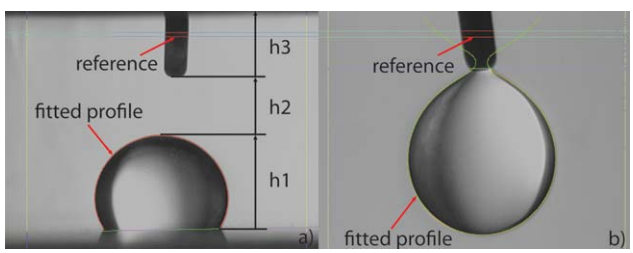

Figure 3. Drop analysis methods.

(a) Sessile drop method (h1 = height of the droplet, h1 + h2 + h3 = height of the aqueous phase layer) and (b) pendant drop method. [Color figure can be viewed in the online issue, which is available at www.interscience.wiley.com.]

A detailed description of the method can be found in a previous work.[13]

$$\frac{d^2z}{dx^2}+\frac{1}{x}\frac{dz}{dx}\left(1+\left(\frac{dz}{dx}\right)^2\right)=\left(\frac{2}{R}-\frac{\Delta\rho gz}{\sigma}\right)\left(1+\left(\frac{dz}{dx}\right)^2\right)^{3/2} \tag{1}$$

In some experiments, the composition of the droplet after a certain time was also measured. The amount of CO_2 dissolved into the droplet was determined volumetrically with the experimental setup presented in Figure 1, according to the following procedure: A drop of organic solvent was submerged into the aqueous phase and the system was subjected to CO_2 pressure as previously described; in this case, the initial volume of the droplet was much higher than in other experiments so a big enough sample of the droplet could be taken for the composition determination. A sample of the drop was taken with a syringe during the experiment and connected to the device presented in Figure 2 through a cold trap, to retain and measure the amount of solvent in the sample. The amount of CO_2 can be derived from the displacement of a column of water by the following expression:

$$X_{CO_2}=\frac{\rho_{CO_2}V_{EXP}}{m_{SAMPLE}} \tag{2}$$

The density of CO_2 was calculated at ambient temperature and ambient pressure in addition to the hydrostatic pressure of the column of water h.

Mathematical model

Model description. For complementing experimental results, a mathematical model of the mass transfer trough the aqueous phase to the droplet has been developed. This model allows calculating the variations in composition and density of the droplet, as well as the mass transfer rates of the different compounds. This model is based on the following assumptions:

- Isothermal and isobaric conditions are assumed.
- Drops are supposed to be spherical.
- As in actual experiments, it is considered that water and dichloromethane phases are in equilibrium before the beginning of the experiment, that is, water has been saturated with dichloromethane, and dichloromethane has been saturated with water.
- The diffusion of water, carbon dioxide, and dichloromethane through the water layer and the mass transfer of these components between the droplet and the water phase are considered. The presence of surfactant is only considered through the possible influence of this compound on the mass transfer coefficients.
- Homogeneous droplet composition is supposed, that is, no radial composition gradients within the droplet are considered. The mass transfer between the droplet and the water phase is described by means of the individual mass transfer coefficients inside the droplet and between the droplet surface and the water phase, being the driving force for the mass transfer the phase equilibrium conditions between the droplet and the water phase.
- In the case of the water phase, radial composition profiles are also not considered, and only the diffusion in the axial coordinate, from the water surface to the bottom of the water layer, where the droplet is located, is taken into account in the calculations.
- It is considered that the surface of the water layer is always in equilibrium with the surrounding gas phase. In the case of CO_2, this supposition implies that its concentration on the water surface is equal to the solubility of CO_2 at the operating pressure and temperature. In the case of dichloromethane, this supposition implies that its concentration in the water surface is equal to zero. This is justified considering the very small amount of dichloromethane used to prepare the sample, which would result in nearly zero concentration in the gas phase even after complete evaporation of all the dichloromethane.
- It is supposed that the height of the water layer is constant during all the experiment, that is, the evaporation of water does not cause a significant reduction of the height of the water layer. This is justified by experimental observations that indicate that this height is indeed nearly constant.
- Because CO_2 and dichloromethane are present in very dilute concentrations in the water phase, the physical properties of this phase are considered constant and equal to those of pure water throughout the experiment. The diffusion of CO_2 and dichloromethane through water is described by means of their respective infinite dilution coefficients.
- The variation of the properties of the droplet throughout the experiment due to variations in its composition is taken into account by using an equation of State model.

With these considerations, the mathematical model is constituted by the equations described in the following paragraphs. The diffusion of CO_2 and dichloromethane through the water phase can be calculated with the following conservation equation[14]:

$$\frac{\partial x_i}{\partial t}=D^0_{i,H_2O}\frac{\partial^2 x_i}{\partial z^2} \tag{3}$$

Initial conditions state that at the beginning of the experiment water is saturated with dichloromethane:

$$t=0\rightarrow x_{CO_2}=0,\quad x_{DCM}=x^{SAT}_{DCM} \tag{4}$$

Boundary conditions at the surface state that there exists phase equilibrium between the water and the gas phase, as previously described:

$$x=0\rightarrow x_{CO_2}=x^{SAT}_{CO_2},\quad x_{DCM}=0 \tag{5}$$

Boundary conditions at the bottom of the water layer result from the mass transfer to the droplet:

$$x=h\rightarrow D^0_{i,H_2O}\frac{\partial x_i}{\partial z}=N_i \tag{6}$$

where the mass flux of each component N_i is calculated as follows:

$$N_i=J_i+\rho\cdot v_t\cdot x_i \tag{7}$$

Table 1. Physical Properties of Materials Considered in this Work

	T_c (K)	P_c (MPa)	w	k
Carbon dioxide	304.2	7.38	0.239	0.04285
Dichloromethane	510.0	6.08	0.199	0.0746
Water	647.3	22.09	0.344	−0.06635

The mass transfer of all components between the droplet and the water phase must fulfill the mass balance:

$$N_i^{H_2O} = N_i^{DROP} = N_i \tag{8}$$

The total convective fluxes at both sides of the interface must also be equal:

$$\rho^{H_2O} v^{H_2O} = \rho^{DROP} v^{DROP} \tag{9}$$

In addition to this, the compositions at the water-droplet interface are interrelated through their phase equilibrium relationship:

$$y_i^* = K_i(T, P, x, y) \cdot x_i^* \tag{10}$$

In these equations, the diffusive mass flux is calculated with the Maxwell–Stefan equations for multicomponent systems:

$$(J) = -\rho[D](\nabla x) \tag{11}$$

where the Maxwell–Stefan diffusivities can be expressed as[14,15]:

$$[D] = [B]^{-1}[\Gamma] \tag{12}$$

In this equation, B takes into account the drag effects, and Γ the thermodynamic effects B can be calculated from the binary diffusivities with the following equations:

$$B_{ii} = \frac{x_i}{D_{in}} + \sum_{\substack{k=1 \\ k\neq i}}^{n} \frac{x_k}{D_{ik}} \qquad i = 1, 2.... \; n-1 \tag{13}$$

$$B_{ij(i\neq j)} = -x_i\left(\frac{1}{D_{ij}} - \frac{1}{D_{in}}\right) \qquad i, j = 1, 2.... \; n-1 \tag{14}$$

And G is calculated as follows:

$$\Gamma_{ij(i\neq j)} = \delta_{ij} + x_i \frac{\partial \ln \hat{\phi}_i}{\partial x_j} \qquad i, j = 1, 2.... \; n-1 \tag{15}$$

The mass balance to each of the three components inside the droplet can be written as follows:

$$\frac{dn_i}{dt} = a^{DROP} \cdot \rho^{DROP} \cdot k_i^{DROP} \cdot \left(y_i - y_i^*\right) \tag{16}$$

The resolution of this set of equations allows calculating the evolution of droplet composition and of all derived properties with time.

Model Parameterization. Density and phase equilibrium of water-carbon dioxide-dichloromethane mixtures has been calculated with the Peng Robinson equation of state with Stryjek–Vera alpha function[16] and Wong–Sandler mixing rules (PRWS EoS).[17] The Stryjek–Vera alpha function improves VLE calculations particularly in mixtures including low-molecular weight compounds, and it requires a component-specific parameter κ which is calculated by correlation of experimental vapor pressure data. On the other hand, Wong–Sandler mixing rules are adequate for the highly nonideal mixture of polar and nonpolar compounds of this application. In this work, the nonrandom two liquid (NRTL) activity coefficient model was used in the mixing rules of the PRWS EoS, as it is shown in Eqs. 17 and 18. Interaction parameters have been correlated to experimental phase equilibrium data by minimization of the difference between experimental and calculated equilibrium pressure, according to the objective function presented in Eq. 19. A detailed description of the procedure used to calculate the parameters of the PRWS EoS for applications with CO_2-H_2O mixtures at high pressures was presented in a previous work.[18]

$$\frac{G^E}{RT} = x_1 x_2 \left(\frac{G_{21}\tau_{21}}{x_1 + x_2 G_{21}} + \frac{G_{12}\tau_{12}}{x_2 + x_1 G_{12}}\right) \tag{17}$$

$$\ln G_{ij} = -\alpha_{ij}\tau_{ij} \tag{18}$$

$$\text{AAPD}\% = \frac{100}{n_{exp}} \sum_{i=1}^{n\,exp} \frac{\left|P_{exp} - P_{calc}\right|}{P_{exp}} \tag{19}$$

Binary interaction parameters of water-carbon dioxide have been calculated by correlation of the data presented by Bamerger et al.[19] These authors measured the vapor-liquid equilibrium of CO_2-H_2O mixtures at temperatures ranging from $T = 323$ K to $T = 353$ K and pressures ranging from $P = 4$ MPa to $P = 14$ MPa, and they reported that their measurements were consistent with previous measurements. Binary interaction parameters of dichloromethane-carbon dioxide have been correlated to the data reported by Stievano and Elvassore.[20] Binary interaction parameters of water-dichloromethane have been correlated using the liquid–liquid phase equilibrium data reported in the DETHERM database.[21] With the correlated parameters, the PRWS EoS reproduces experimental data of the carbon dioxide-water system with AAPD% = 2.0%, of the carbon dioxide-dichloromethane system with AAPD% = 6.9%, and of the water-dichloromethane system with AAPD% = 9.7%. The obtained binary interaction parameters as well as pure component properties are presented in Tables 1 and 2.

Table 2. Interaction Parameters for the PRWS EoS

	CO_2-DCM	CO_2–H_2O	DCM-H_2O
$k_{12} = k_{21}$	0.4292	0.3073	0
t_{12}	0	4.3870	5.0180
t_{21}	0	0.3930	5.0180
$a_{12} = a_{21}$	0	0.1141	0.2007

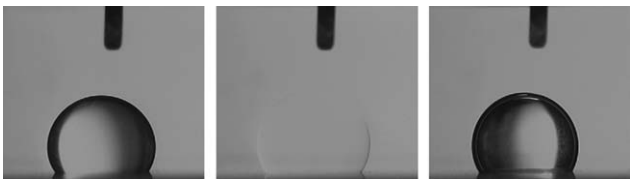

Figure 4. Refractive index changes during a typical experiment.

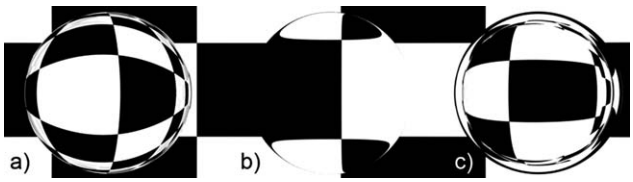

Figure 5. Simulated refractive index effect of a sphere with a relative refractive index: (a) higher, (b) almost equal, and (c) lower than its surrounding medium.

Accurate density calculations are particularly important in this case because they provide the link between the observable variations of volume of the droplet and the calculated droplet compositions, which are the main result of the model. The PRWS EoS has also been used to calculate the density of the droplet as a function of composition, temperature and pressure. A volume translation V^t has been used to improve density calculations, which is defined according to Eq. 18. For CO_2, the volume translation has been calculated as a function of temperature and pressure using the Magoulas and Tassios correlation.[22] For water and dichloromethane, a constant volume translation has been used, calculated by adjustment of the equation to experimental density data of the saturated liquid at atmospheric conditions. These volume translation corrections were 2.4751×10^{-6} m^3/mol for dichloromethane, and 3.7103×10^{-6} m^3/mol for water. With this method, the equation reproduced the saturated liquid density of carbon dioxide-dichloromethane mixtures (which are the two main constituents of the droplet) reported by Stievano and Elvassore[20] with AAD% = 2.4%.

$$V^{\text{corr}} = V^{\text{EoS}} - V^{\text{t}} \tag{20}$$

The infinite dilution diffusion coefficients of CO_2 and dichloromethane in water have been calculated as a function of temperature using the Hayduk–Minhas correlation for aqueous solutions.[23] Because the concentration of both dichloromethane and CO_2 in the water layer is very low (in the order of $x = 10^{-2}$ in molar fraction, limited by solubility), the composition dependence of diffusion coefficients has been neglected and they have been considered constant and equal to the infinite dilution coefficients.

Inside the droplet and in the droplet interface, the supposition of infinite dilution is not valid and the composition dependence of diffusion coefficients has to be taken into account. The dependence of the diffusion coefficients on the composition was calculated with the method proposed by Kooijman and Taylor for multicomponent systems[24]:

$$D_{ij} = \left(D_{ij}^0\right)^{xj}\left(D_{ji}^0\right)^{xi}\prod_{\substack{k=1\\k\neq i,j}}^{n}\left(D_{ik}^0 D_{jk}^0\right)^{xk/2} \tag{21}$$

Infinite dilution diffusion coefficients of carbon dioxide-dichloromethane-water mixtures inside the droplet were estimated with the Tyn and Calus method.[23]

With these values of diffusivities, individual mass transfer coefficients have been calculated using the well-known equation $Sh = 2$ for diffusion to spheres.[23]

Model Resolution. To solve the model equations the partial differential equation, which describes the diffusion in the water phase, Eq. 3, has been transformed into a system of ordinary differential equations (ODEs) by using a central finite difference scheme. This system of ODEs, together with the differential mass balances inside the droplet, Eq. 16, have been numerically integrated using the ODE solver implemented in the built-in ode45 function of Matlab® 7.0.

Results and Discussion

Dichloromethane-carbon dioxide-water system

The volume behavior of the system dichloromethane-carbon dioxide-water was analyzed at two different conditions: first at a pressure of 5 MPa and temperature of 308 K where CO_2 is a compressed gas, and then at a pressure of 10 MPa and temperature of 308 K where CO_2 is a supercritical fluid. Additionally, different initial volumes of the drops were tested and the resulting volume changes were analyzed.

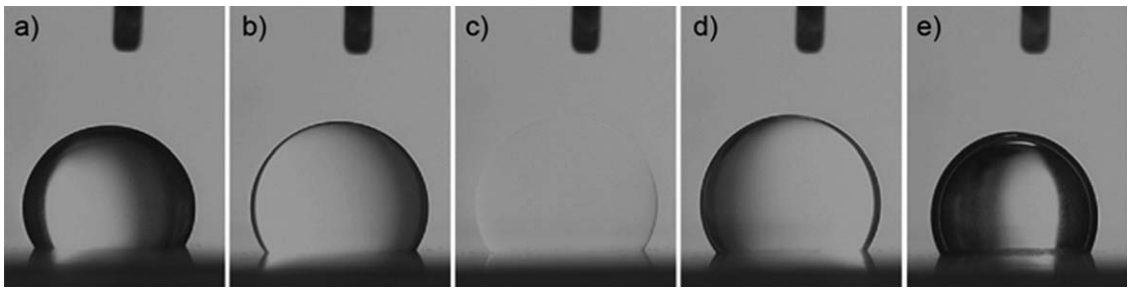

Figure 6. Drop evolution in an experiment at a pressure of 5 MPa and temperature of 308 K.

A video clip is provided as Supporting Information material.

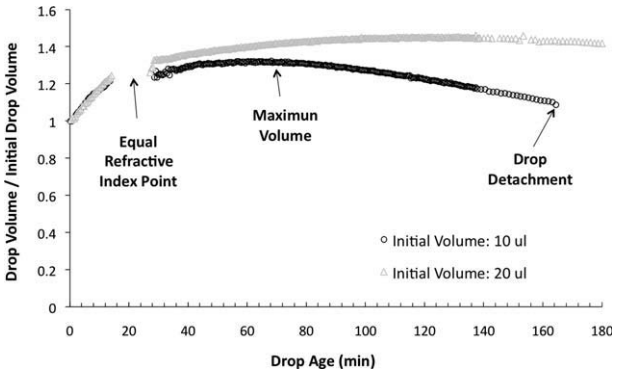

Figure 7. Drop volume evolution in experiments at a pressure of 5 MPa and temperature of 308 K with different initial drop volumes.

In all the experiments, the dissolution of CO_2 into the droplet produced a change in the refractive index. The initial refractive index of the drop consisting on dichloromethane saturated with water at 308 K was higher than the refractive index of the surrounding medium. However, through the experiment, the refractive index of the drop changed to values below the ones of the surrounding medium going through a point were both refractive indexes were nearly the same and the drop became almost invisible for the CCD-camera. Figure 4 presents snapshots taken at different times of a typical experiment showing the effect of changes in refractive index on the drop visualization.

The refractive index effect for a sphere with higher, equal and lower refractive index than its surrounding media are presented in Figure 5, to compare with those from the experiments. Although this effect could be considered as a drawback for the measuring method, it is also a characteristic point in the experiments, which may give an easily observable indication of the droplet composition. Therefore, the measurements of droplet composition were focused in determining it at the moment of equal refractive index. In experiments performed at pressures of 5 MPa and temperature of 308 K, the measured concentration of CO_2 in the drop was $5.97 \pm 0.02\%$ in weight basis.

With respect to the evolution of drop volume with time, different behaviors were observed in the experiments at 5 and 10 MPa. At the lower pressure, the volume of the drop first increased until it reached a maximum value and then decreased until the drop was detached from the bottom of the cell. Figure 6 shows a sequence of images of a typical experiment at 5 MPa, (a) first the initial state of the drop before the CO_2 is introduced in the cell, (b, c) the change in the refractive index already described and the point where the refractive index of the drop and medium become equal, (d) the maximum volume point, and (e) the volume reduction and detachment of the drop. Figure 7 shows the variation of droplet volume with time in experiments performed at 5 MPa with different initial drop volumes. A video-clip showing the evolution of the drop during the experiment corresponding to Figure 6 is provided as Supporting Information material.

On the other hand, in the experiments carried out at 10 MPa, the volume of the drop continuously increased until the drop got detached from the bottom of the cell. Figures 8 and 9 show the evolution of the drop's volume in a typical experiment performed at a pressure of 10 MPa and temperature of 308 K, where (a) the initial state of the drop, (b) the point where the refractive index of the drop and surrounding media match, (c) the increase of the drop volume, and (d) the detachment of the drop are depicted. A video-clip showing drop evolution in this experiment is provided as Supporting Information material.

The different behaviors in these experiments are explained by the phase behavior of carbon dioxide-water-dichloromethane mixtures. In the experiments performed at a pressure of 5 MPa, the pressure is below the mixture critical point pressure of carbon dioxide-dichloromethane mixtures,[20] and the solubility of carbon dioxide is 0.0137 (molar fraction).[19] In contrast, in the experiments performed at 10 MPa, pressure is above the mixture critical pressure of carbon dioxide-dichloromethane mixtures, and CO_2 solubility in water is 0.0205 (molar fraction). Therefore, in the experiments performed at 5 MPa, the diffusion of CO_2 to the drop is limited both by the equilibrium concentration of carbon dioxide-dichloromethane mixtures and the lower solubility of CO_2 in water. As the experiment progresses and CO_2 concentration into the drop increases, these equilibrium constraints tend to slow down CO_2 diffusion into the droplet, until the volume variation becomes negative due to the comparatively faster diffusion of dichloromethane out of the droplet.

In the experiments performed at 10 MPa, CO_2 diffusion is not so limited by equilibrium conditions and drop swelling due to CO_2 diffusion prevails over drop shrinking due to dichloromethane diffusion out from the drop. Thus, drop volume increases continuously until the density of the drop is

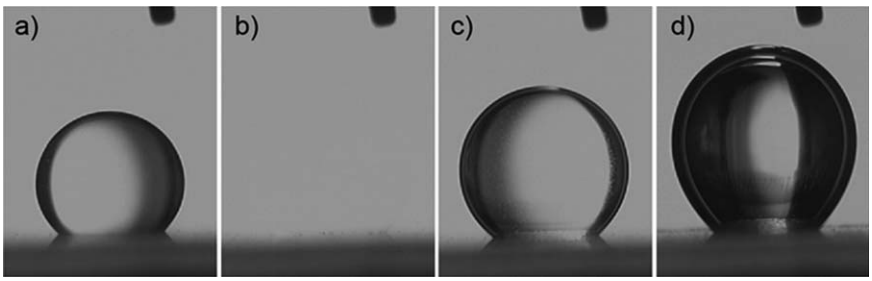

Figure 8. Drop evolution in an experiment at a pressure of 10 MPa and temperature of 308 K.

A video clip is provided as Supporting Information material.

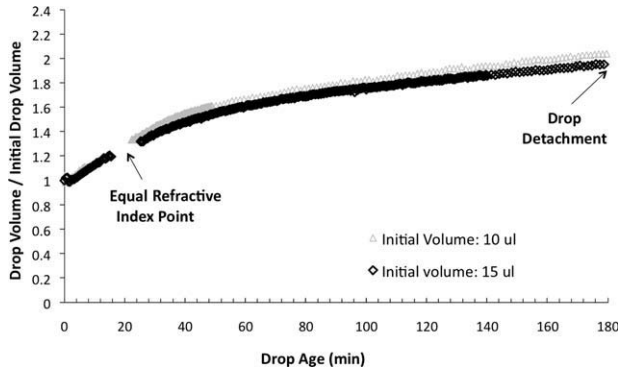

Figure 9. Drop volume evolution in experiments at a pressure of 10 MPa and temperature of 308 K with different initial drop volumes.

low enough to compensate the attachment effect of the cell surface and it ascends to the surface of the aqueous phase.

Dichloromethane-carbon dioxide-water + starch-based surfactant system

Several experiments were performed adding an (OSA)-modified starch surfactant to the aqueous phase. This is the same surfactant used to stabilize the emulsions for the SFEE for β-carotene precipitation.[11] The aim of these experiments was to determine if carbon dioxide has a negative effect over the tensoactive properties of the modified starch surfactant, and if the presence of the surfactant had an influence on the mass transfer. The experiments were carried out at a temperature of 308 K and pressures of 5 and 10 MPa. The surfactant was added to the presaturated phases of dichloromethane with water and water with dichloromethane with a concentration above the critical micelle concentration.

Figure 10 shows the comparison between the volume changes relative to the initial volume of the drop, in an experiment with a drop surfactant concentration of 0.5 g/L

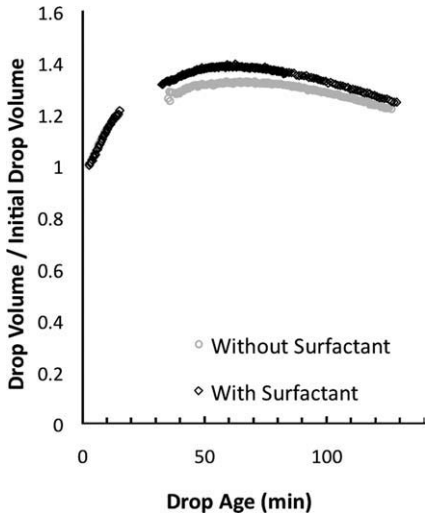

Figure 10. Drop volume evolution in experiments at a pressure of 5 MPa and temperature of 308 K with modified starch OSA surfactant concentration of 0.5 g/L.

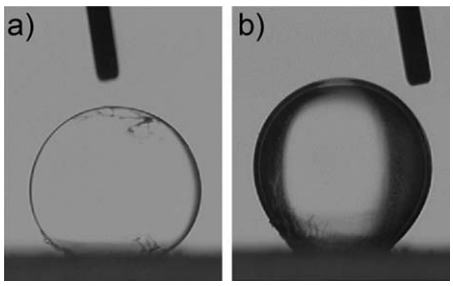

Figure 11. Surfactant precipitation in an experiment performed with an initial surfactant concentration of 1 g/L.

and for a drop without surfactant. It can be seen that the effect of the surfactant on the transport of CO_2 and dichloromethane is minor.

To observe if CO_2 could precipitate the surfactant and affect its properties, an experiment with a higher concentration of surfactant was performed. One gram per liter of the modified starch (OSA) was dissolved in the water, and since this value exceeded the solubility in the organic solvent phase at the desired temperature conditions, a dichloromethane rich phase saturated with the surfactant was used instead.

When the CO_2 was added the surfactant dissolved in the organic solvent precipitated and large particles were formed migrating to the interface between the drop and the medium and between the drop and the cell surface. Figure 11 illustrates the surfactant particles formed during those experiments.

Dichloromethane + β-carotene-carbon dioxide-water system

Experiments at pressures of 5 and 10 MPa and a temperature of 308 K were carried out for the dichloromethane-water-carbon dioxide system containing β-carotene dissolved in the dichloromethane drop. The precipitation of the β-carotene within the drop was obtained and several small particles were formed during the first moments of the experiments, as it can be observed in the video-clip provided as Supporting Information material. Figure 12 shows the particles formed inside the drop at different times for a pressure of 5 MPa and temperature of 308 K. The same behavior was observed for the system at 10 MPa and 308 K. However differences were observed on the amount of dichloromethane in the final condition of the experiment as is shown in Figure 13d. The same behavior of emulsion droplets can be expected during SFEE precipitation process, although in a shorter time interval because the conditions and equipment of SFEE processes are designed to improve the mass transfer between emulsion and supercritical solvent (production of emulsions with organic solvent droplets sizes in the range of nanometers, atomization of the emulsion inside carbon dioxide as small droplets, etc.). These experiments demonstrate that in the SFEE process, each drop behaves as a miniature gas antisolvent precipitator, which justifies the ability to control the final particle size by modification of the initial drop size claimed for this process.

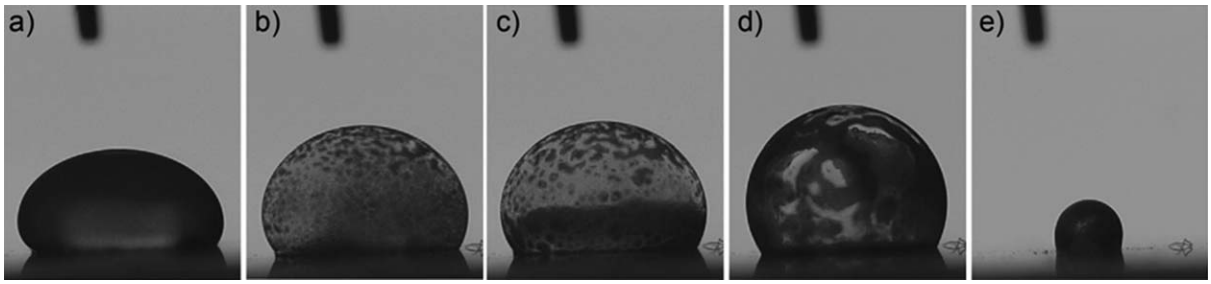

Figure 12. β-carotene particle precipitation during an experiment at pressure of 5 MPa and temperature of 308 K: (a) initial condition, (b) beginning of particle formation, (c, d) particle agglomeration, and (e) final condition after the drop detachment from the cell surface.

Mass transfer model results

Figure 14 shows a comparison of the experimental volume variation curve obtained in an experiment performed at 10 MPa with the model results. Two calculated curves are presented in this figure: in one of them, the resistance to mass transfer caused by diffusion in the water layer is considered, and in the other this resistance is neglected. It can be seen that there is a reasonably good agreement between experiments and calculations when diffusion in the water layer is neglected. However, when this resistance is considered, the increase of calculated droplet volume with time is much slower than the increase observed in the experiments. In particular, according to model results due to the diffusion in the water layer there is a delay between the beginning of the experiment and the time at which droplet volume begins to grow, indicated by the sigmoidal shape of the curve. While in the experiments, a fast increase in drop volume is observed already at the beginning of the experiment. This indicates that there is a faster mechanism for the mass transfer of CO_2 and dichloromethane through the water layer than molecular diffusion, which is the mechanism considered in the model. A possible explanation for this difference is that the stirring of the water layer caused by the pressurization with CO_2 causes a fast saturation of water with CO_2 at the beginning of the experiment. Other possible reasons are the natural convection streams and interfacial turbulence due to Marangoni effect, which are known to occur in CO_2-H_2O systems because the density of CO_2-saturated water is higher than that of pure water.[25,26] The same observations can be done with respect to the comparison of experimental and model results at 5 MPa, presented in Figure 15. Even without considering the resistance to mass transfer in the water layer, the volume predicted by the model is slightly slower than experimental observations. This could be due to the interfacial turbulence phenomenon that can take place in multicomponent systems.[13]

Figures 16 and 17 present model results concerning the evolution of droplet composition and density, at a pressure of 10 MPa. The results presented in these figures were obtained neglecting the resistance to mass transfer caused by diffusion in the water layer. The times at which the equal refractive index phenomenon and the droplet detachment are observed are also indicated in these figures.

In Figure 16, it can be seen that the concentration of CO_2 in the droplet constantly increases as the experiment proceeds, reaching molar fractions above 0.9 when drop detachment occurs. Extrapolation with the model indicates that if drop detachment could be prevented, CO_2 concentration in the drop would continue increasing until the limiting value $X_{CO_2} = 1$. The calculated droplet composition in the period of equal refractive index is $X_{CO_2} = 0.18$ (molar fraction), equivalent to a mass fraction of 10%, which is higher than the value of 6% experimentally determined. This observation indicates that model overpredicts the rates of diffusion of CO_2 into the droplet and of dichloromethane out of the droplet. Calculated droplet density when droplet detachment

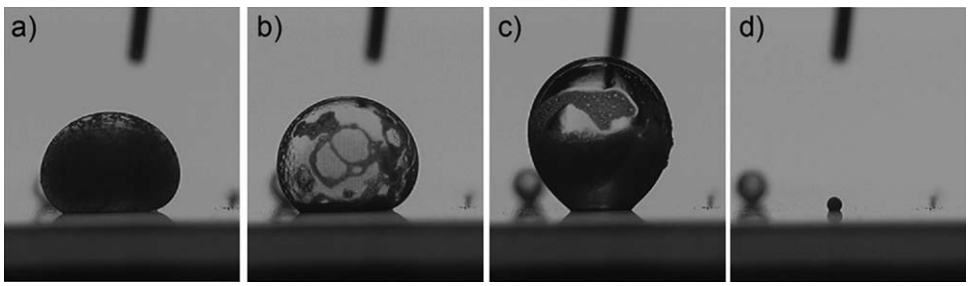

Figure 13. β-carotene particle precipitation during an experiment at pressure of 10 MPa and temperature of 308 K: (a) beginning of particle formation, (b, c) particle agglomeration, and (d) final condition after the drop detachment from the cell's surface.

A video clip is provided as Supporting Information material.

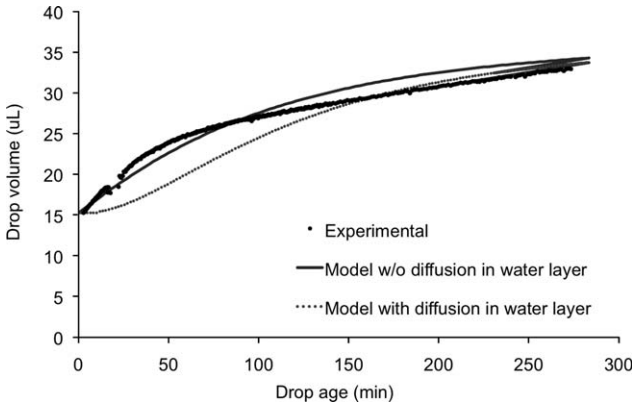

Figure 14. Drop volume evolution vs. drop age in an experiment at pressure of 10 MPa and temperature of 308 K, experimental and model results.

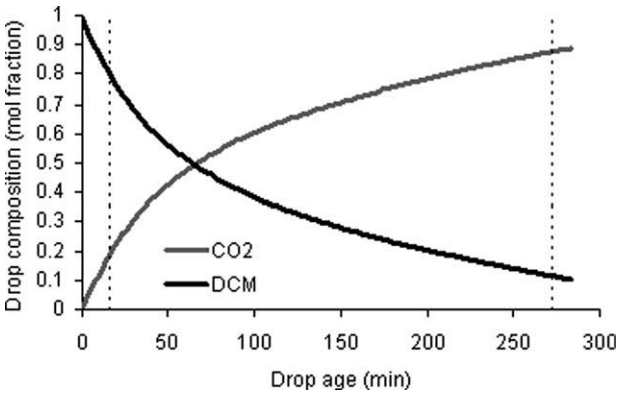

Figure 16. Calculated drop composition evolution as a function of drop age.

Pressure of 10 MPa and temperature of 308 K. Vertical dashed lines indicate the times at which equal refractive index and drop detachment are observed.

occurs is 0.985 g/mL; the lower density of the drop with respect to water is responsible for droplet detachment by flotation in this point. Similar results are obtained with the simulations performed setting a pressure of 5 MPa.

Interfacial tension measurements

Figure 18 shows the evolution of the interfacial tension as a function of time in two experiments carried out at pressures of 5 and 10 MPa, respectively. These interfacial tensions were obtained by the image analysis software by application of Eq. 1 as previously described. For this, the density of the two phases, which is a function of their composition, is required. The mean density of the aqueous phase can be considered constant with time as the density of an aqueous phase saturated with CO_2 at the same temperature and pressure of the experiment. The density of the drop phase changes with variations in the composition of CO_2. The model results obtained for the sessile experiments showed that the composition of CO_2 in the drop has an intense increase initially and it could be considered linear with time, as it is shown in Figure 16. Knowing the composition of the drop in the equal refractive index point allows the calculation of a linear composition variation until that point. The PRWS EoS with a volume translation has been used to calculate drop density as a function of composition.

An increase in the interfacial tension of ~20 mN/m was observed during the first 10 min of the experiments with a temperature of 308 K and pressures of 5 and 10MPa. Determination of interfacial tensions at longer times were hindered first by the phenomenon of the equal refractive index point, and then by the approximation of the density of the aqueous and the organic phase, which caused the drop to adopt a nearly spherical shape and rendered measurements very inaccurate.

The effect of the composition of a liquid on the interfacial tension can be explained by means of the Gibbs–Duhem equation which, in the case of an isothermal and isobaric diluted binary system can be expressed with Eq. 22.

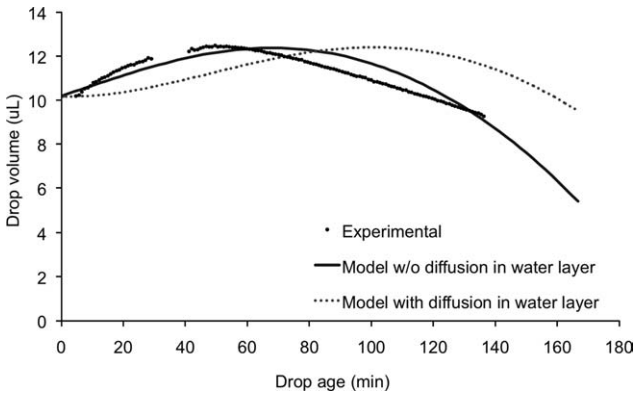

Figure 15. Drop volume evolution vs. drop age in an experiment at pressure of 5 MPa and temperature of 308 K, experimental and model results.

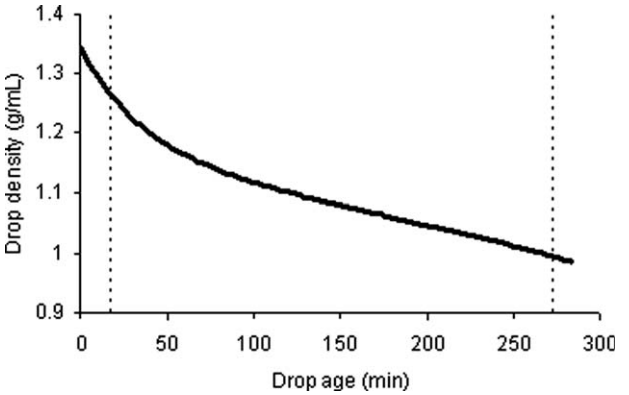

Figure 17. Calculated drop density evolution as a function of drop age.

Pressure of 10 MPa and temperature of 308 K. Vertical dashed lines indicate the times at which equal refractive index and drop detachment are observed.

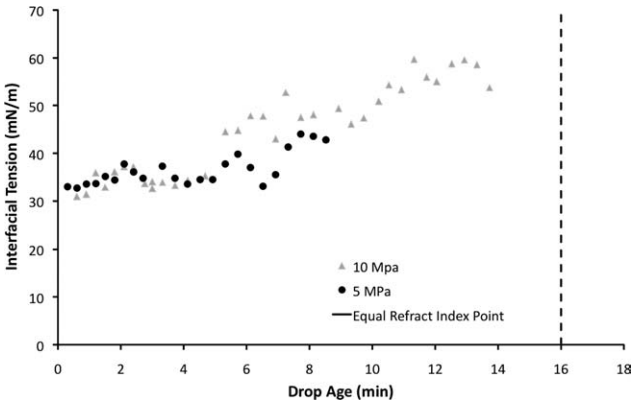

Figure 18. Interfacial tension evolution curve of the system DCM-H_2O-CO_2 at 308 K at 5 and 10 MPa.

$$d\sigma = -\Gamma_2^{(1)} RTd\ln(x_2) \tag{22}$$

The indices 1 and 2 represent the two compounds that form the coexisting phases. The excess concentration Γ_i is the mole amount n_i per unit of area A. Equation 22 describes the effect of changes in mass transport of the components between phases. The minus algebraic sign on the right hand of the equation indicates that adsorption of one of the components, and the consequent increase of that component fraction x_i, on the interface causes a decrease in the interfacial tension. On the other hand, desorption effects causes an increase in the interfacial tension. A detailed description of the concentration effect over the interfacial tension is treated by Sutjiadi-Sia et al.[13]

During the experiments diffusion of CO_2 from the aqueous phase into the drop and of dichloromethane out from the drop occurs. Each transport affects the interfacial tension of the coexisting phases in opposite way according to the Gibbs law. However, desorption of dichloromethane determines the variation of the interfacial tension as shown in Figure 18. The same behavior was observed by Sutjiadi-Sia et al.[13] in the study of water + ethanol drops in high-pressure carbon dioxide.

Because the interfacial tension increases as a result of CO_2 mass transfer to the drop, it is expected that the emulsion will become less stable under CO_2 pressure. This is in agreement with the results of Varona et al.,[27] who observed that a lavandin oil-in-water emulsion would become unstable after a few minutes of exposition to high-pressure carbon dioxide, while the same emulsion was stable for several weeks under atmospheric conditions.[28] This effect can be a hindrance for processes, which involve a long residence time of the emulsion in the SC-CO_2 environment, like the batch supercritical fluid extraction of emulsions process.

Conclusions

The experimental results presented in this work demonstrate that during the supercritical fluid extraction of emulsions process each organic solvent drop behaves as a miniature gas antisolvent precipitator. Supercritical carbon dioxide diffuses through the aqueous phase to the drop, causing a considerable drop swelling. Depending on the operating pressure and the corresponding carbon dioxide solubility in the aqueous and organic phases, the swelling caused by CO_2 can be overcome by the diffusion of dichloromethane out of the drop, and thus drop shrinking is observed after a certain time in the experiments performed at moderate pressures (5 MPa). A mathematical model has been developed to describe CO_2 and dichloromethane diffusion and the associated drop volume changes. Model results show that CO_2 concentration inside the drop can be as high as 0.9 (mol fraction) before drop detachment by flotation occurs. When a solute like β-carotene is dissolved into the organic phase, precipitation occurs due to the antisolvent effect of the carbon dioxide that diffuses to the drop, and many small β-carotene particles are formed inside the drop. When the concentration of surfactant is high, it can also precipitate due to the antisolvent effect of CO_2. In both cases, the produced particles tend to migrate to the drop interface.

Interfacial tension measurements show that interfacial tension increases due to the diffusion of dichloromethane out of the drop. This increase in the interfacial tension has a destabilizing effect on the emulsion that can have important implications for applications that involve long contact of the emulsion with the supercritical fluid. The measured increase of the interfacial tension is in agreement with the destabilization effect of supercritical carbon dioxide over similar oil-in-water emulsions.

Acknowledgments

This work was supported by the Spanish Ministry of Science and Education CTQ2006-02099, and by the EU Marie Curie ERT EPSS 007767 PROBIOMAT project. The technical assistance and the materials provided by Vitatene S.A. (León, Spain) and by National Starch Food Innovation (Hamburg, Germany) are gratefully acknowledged. F. Mattea thanks the Spanish Ministry of Education for an FPU grant and for financing his research stay in the Hamburg University of Technology (Germany). A. Martín thanks the Alexander von Humboldt foundation (Germany) for a postdoctoral research fellowship.

Notation

a = drop interfacial area (m^2)
AAPD% = average absolute pressure deviation (Eq. 17)
B = Maxwell–Stefan drag factor (s/m^2)
D_{ij} = diffusivity (m^2/s)
g = gravity (m/s^2)
h = height of the aqueous phase layer (m)
J_i = diffusive flow of component i (mol/s)
k_i = transfer coefficient of component i (m^2/s)
k_{ij} = binary interaction coefficient between components i and j
K_i = phase equilibrium distribution coefficient of component i
M = mass (g)
n_{exp} = number of experimental data points
N_i = molar flow of component i (mol/s)
P = pressure (Pa)
P_c = critical pressure (Pa)
R = drop radius (m)
t = time (s)
T = temperature (K)
T_c = critical temperature (K)
V = volume (m^3)
V^t = volume correction (Eq. 18) (m^3)
v_t = interface velocity (m/s)
x = drop composition (mol fraction)

y = Aqueous phase composition (mol fraction)
z = Axial coordinate (m)
α_{ij} = interaction parameter, Wong–Sandler mixing rules
G = Maxwell–Stefan thermodynamic factor
κ = Stryjek–Vera alpha function constant
ρ = density (mol/m^3)
σ = interfacial tension (mN/m)
τ_{ij} = interaction parameter, Wong–Sandler mixing rules
ω = acentric factor

Literature Cited

1. Moraru CI, Panchapakesan CP, Huang Q, Takjistov P, Liu S Kokini JI. Nanotechnology: a new frontier in food science. *Food Technol.* 2003;57:24–29.
2. Grau MJ, Kayser O, Muller RH. Nanosuspensions of poorly drugs-reproducibility of small scale production. *Int J Pharm.* 2000;196: 155–157.
3. Mullin JW.*Crystallization*, 4th ed. Oxford, UK.: Butterworth-Heineman, 2001.
4. Avalos J, Cerdá-Olmedo E. *Fungal carotenoid production*. In: Arora DK, editor. *Handbook of Fungal Biotechnology*, 2nd ed., Vol. 1. New York: Marcel Dekker, Inc., 2004: 367–378.
5. Horn D, Rieger J. Organic nanoparticles in the aqueous phase—theory, experiment and use. *Angew Chem Int Ed.* 2001;40:4330–4361.
6. Mattea F, Martín A, Cocero MJ. Carotenoid processing with supercritical fluids. *J Food Eng.* 2009;93:255–265.
7. Mattea F, Martín A, Cocero MJ. Co-precipitation of β-carotene and polyethylene glycol with compressed CO_2 as an antisolvent: effect of temperature and concentration. *Ind Eng Chem Res.* 2008;47: 3900–3906.
8. Miguel F, Martín A, Mattea F, Cocero MJ. Precipitation of lutein and co-precipitation of lutein and poly-lactic acid with the supercritical anti-solvent process. *Chem Eng Proc.* 2008;47:1594–1602.
9. Shekunov BY, Chattopadhyay P, Seitzinger J, Huff R. Nanoparticles of poorly water-soluble drugs prepared by supercritical fluid extraction of emulsions. *Pharm Res.* 2006;23:196–204.
10. DellaPorta G, Reverchon E. Nanostructured microspheres produced by supercritical fluid extraction of emulsions, *Biotechnol Bioeng.* 2008;100:1020–1033.
11. Mattea F, Martín A, Cocero MJ. Supercritical antisolvent precipitation from an emulsion: β-carotene nanoparticle formation. In: *Proceedings of 9th International Symposium on Supercritical Fluids*, Barcelona, Spain. 2009.
12. Bashforth F, Adams JC. *An Attempt to Test the Theories of Capillary Action by Comparing the Theoretical and Measured Forms of Drops of Liquids with an Explanation of the Method of Integration Employed in Constructing the Tables Which Give the Theoretical Forms of Such Drops*. Cambridge, Cambridge, UK. 1883.
13. Sutjiadi-Sia Y, Jaeger P, Eggers R. Interfacial phenomena of aqueous systems in dense carbon dioxide. *J Supercrit Fluids.* 2008;46: 272–279.
14. Bird RB, Stewart WE, Lightfoot EN. *Transport Phenomena*, 2nd ed. New York: Wiley, 2001.
15. Deen WM. *Analysis of Transport Phenomena*. USA: Oxford University Press, 1998.
16. Stryjek R, Vera JH. PRSV—an improved Peng-Robinson equation of state with new mixing rules for strongly nonideal mixtures. *Can J Chem Eng.* 1986;64:334–340.
17. Wong DS, Sandler SI. A theoretically correct mixing rule for cubic equations of state. *AIChE J.* 1992;72:671–680.
18. Martín A, Bouchard A, Hofland GW, Witkamp G-J, Cocero MJ. Mathematical modelling of the mass transfer from aqueous solutions in a supercritical fluid during particle formation. *J Supercrit Fluids.* 2007;44:126–137.
19. Bamerger A, Sieder G, Maurer G. High-pressure (vapor + liquid) equilibrium in binary mixtures of (carbon dioxide + water or acetic acid) at temperatures from 313 to 353 K. *J Supercrit Fluids.* 2000; 17:97–110.
20. Stievano M, Elvassore N. High-pressure density and vapor-liquid equilibrium for the binary systems carbon dioxide-ethanol, carbon dioxide-acetone and carbon dioxide-dichloromethane. *J Supercrit Fluids.* 2005;33:7–14.
21. *DETHERM, Thermophysical Property Data Base*. Available at: http://cds.dl.ac.uk/cds/datasets/physchem/detherm/detherm.html Accessed April 25, 2009.
22. Magoulas C, Tassios D. Thermophysical properties of n-alkanes from C1 to C20 and their prediction for higher ones. *Fluid Phase Eq.* 1990;56:119–140.
23. Poling BE, Prausnitz J, O'Connell JP. *The Properties of Gases and Liquids*, 5th ed. New York: McGraw-Hill, 2001.
24. Kooijman HA, Taylor R. Estimation of diffusion coefficients in multicomponent liquid systems. *Ind Eng Chem Res.* 1991;30:1217–1222.
25. Yang C, Gu Y. Accelerated mass transfer of CO_2 in reservoir brine to density-driven natural convection at high pressures and elevated temperatures. *Ind Eng Chem Res.* 2006;45:2430–2436.
26. Arendt B, Dittmar D, Eggers R. Interaction of interfacial convection and mass transfer effects in the system CO_2-water. *Int J Heat Mass Transfer.* 2004;47:3649–3657.
27. Varona S, Kareth S, Cocero MJ. Encapsulation of essentials oils using biopolymers for their use in ecological agriculture. In: *Proceedings of 9th International Symposium on Supercritical Fluids*, Barcelona, Spain 2009.
28. Varona S, Martín A, Cocero MJ. Formulation of a natural biocide based on lavandin essential oil by emulsification using modified starches. *Chem Eng Proc.* 2009;48:1121–1128.

Manuscript received May 25, 2009, and revision received July 22, 2009.